Journal of Alloys and Compounds 509 (2011) 6539–6544

Contents lists available at ScienceDirect

Journal of Alloys and Compounds

journal homepage: www.elsevier.com/locate/jallcom

Phase and luminescent intensity control of hydrophilic rare-earth up-converting nanophosphors prepared by one-pot solvothermal synthesis

Yuelin Song[a], Qiwei Tian[a], Rujia Zou[a], Zhigang Chen[a,*], Jianmao Yang[b], Junqing Hu[a,*]

[a] State Key Laboratory for Modification of Chemical Fibers and Polymer Materials, College of Materials Science and Engineering, Donghua University, 2999 North Renmin Road, Shanghai 201620, China
[b] Research Center for Analysis and Measurement, Donghua University, Shanghai 201620, China

ARTICLE INFO

Article history:
Received 23 November 2010
Received in revised form 19 February 2011
Accepted 19 March 2011
Available online 29 March 2011

Keywords:
Rare-earth up-converting nanophosphors
Solvothermal synthesis
Phase
Luminescent intensity

ABSTRACT

Rare-earth up-converting nano-phosphors (RUNPs) have wide applications, and most of these applications require hydrophilic RUNPs with high up-converting luminescence efficiency. In this work, we report a simultaneous control of the phase and luminescent intensity of hydrophilic Gd^{3+} doped $NaYF_4$:Yb/Er nanoparticles with diameters of 40–100 nm, which were prepared by a facile one-pot solvothermal synthesis with ethylene glycol as the solvent and poly(vinylpyrrolidone) as the ligands at 220 °C for different time. When reaction time is 3 h, the increase of Gd^{3+} dopant concentration from 0 to 30 mol% results in the transformation from cubic to hexagonal phase, and pure hexagonal phase $NaYF_4$:Yb/Er nanoparticles can be obtained with Gd^{3+} dopant concentration up to 30 mol%. Gd^{3+} dopant concentration at 15 mol% leads to a maximal luminescent intensity in a wide dopant range of 0–80 mol%. Furthermore, the increase of reaction time from 3 to 24 h favors the formation of hexagonal phase samples and therefore improves greatly luminescence intensity. 15 mol% Gd^{3+} doped $NaYF_4$:Yb/Er nanoparticles prepared for 24 h exhibit the highest upconverting luminescence intensity which is almost 11 times as strong as that of ones prepared for 3 h and almost 28 times as strong as that of hexagonal phase $NaGdF_4$:Yb/Er (namely $NaYF_4$:Yb/Er sample with 80 mol% Gd^{3+} prepared for 3 h). Due to its small size, high hydrophilicity and excellent up-converting luminescence, this 15 mol% doped $NaYF_4$:Yb/Er sample has great superiority for biological applications.

1. Introduction

Upconversion luminescence is a process where low-energy light, usually near-infrared (NIR) or infrared (IR), is converted to higher-energy light (UV or visible), through multiple photon absorptions or energy transfers [1–3]. Rare-earth up-converting nano-phosphors (RUNPs) have attracted increasing attention because of their potential applications in solid-state lasers [4], flat-panel displays [5], solar cells [6], and optical-fiber-based telecommunications [7]. As for biological applications, RUNPs have exhibited many advantages over conventional downconversion fluorescent materials (dyes and quantum dots), such as sharp absorption and emission lines, superior photostability, high chemical stability, low toxicity, noninvasive and deep penetration of NIR radiation, and the absence of autofluorescence of biological tissues [2,3,8]. Very recently, based on up-converting luminescent properties of RUNPs and deep penetration of NIR radiation in biological tissues, our group has reported a 980-nm laser-driven photovoltaic cell as a kind of novel biological electrical source [9]. Generally, most of these applications require hydrophilic RUNPs with high NIR to visible up-converting luminescence efficiency.

For obtaining hydrophilic RUNPs, two types of synthetic strategies have typically been developed. Strategy one is two-step controllable synthesis, and the first step is to prepare RUNPs with hydrophobic organic ligands (such as oleic acid, oleylamine) coating their surface, for example, by the hydrothermal route assisted with oleic acid or linoleic acid [10–13], thermolysis of rare-earth trifluoroacetate [14–16], or some other reaction systems [17–20]. The second step is to convert the hydrophobic RUNPs into hydrophilic ones, for example, by SiO_2/amphiphilic copolymer encapsulation [21,22], ligand exchange [15,20], layer by layer assembly [23]. We have also developed a simple and versatile strategy for converting hydrophobic RUNPs into water-soluble and carboxylic acid-functionalized analogues by directly oxidizing oleic acid ligands to azelaic acid [8]. Strategy two is one-pot synthesis of hydrophilic RUNPs, for example, by hydrothermal synthesis assisted with hydrophilic polymer [24,25], reverse microemulsion-solvothermal route [26] and high temperature synthesis with ethylene glycol as the solvent [27], or glycol-mediated solvothermal synthesis [28]. However, luminescence efficiencies of

---

* Corresponding authors. Fax: +86 21 67792855.
E-mail addresses: zgchen@dhu.edu.cn (Z. Chen), hu.junqing@dhu.edu.cn (J. Hu).

0925-8388/$ – see front matter © 2011 Elsevier B.V. All rights reserved.
doi:10.1016/j.jallcom.2011.03.122

these hydrophilic RUNPs are not well optimized and thus are still unsatisfied.

For obtaining RUNPs with high up-converting luminescence efficiency, some effective ways have been adopted, for example, by tuning host material, crystal phase, size, structure, dopant and surface ligand [2,29–32]. Until now, $NaYF_4$ has been reported to be one of the most efficient host materials for RUNPs, and particularly hexagonal phase $NaYF_4$ exhibits about an order-of-magnitude enhancement of up-converting luminescence efficiency relative to its cubic phase counterpart [2,15,33]. However, hexagonal phase $NaYF_4$ typically exists in bulk materials and large sized particles (size: several μm) [15,34]. Although hexagonal phase $NaYF_4$ nanocrystals (size: <100 nm) have been synthesized by the thermolysis of rare-earth trifluoroacetate in organic solvents [14,15], the synthesis require toxic organometallic precursors and hazardous coordinating solvents. Very recently, Liu et al. [35] reported that Gd^{3+} ion doping approach results in a simultaneous control of phase, size, and luminescence of $NaYF_4$, and ultra-small (~10 nm) hexagonal phase $NaYF_4$ nanocrystals can be fabricated via oleic acid-assisted hydrothermal process. However, all these obtained $NaYF_4$ nanocrystals with efficient up-converting luminescence are hydrophobic, and therefore surface functionalization as the second step is still necessary in many applications because of their very low solubility in water and unfavorable surface properties [36].

Therefore, it is necessary to develop simple methods for the one-pot preparation of hydrophilic RUNPs with high up-converting luminescence efficiency. In the present work, we report a facile one-pot solvothermal synthesis of hydrophilic Gd/Yb/Er co-doped $NaYF_4$ nanocrystals by using ethylene glycol as the solvent and poly(vinylpyrrolidone) (PVP) as the ligand. We find that Gd^{3+} doping concentration and solvothermal time have no obvious effect on their sizes but have strong effect on their phase and luminescent intensity. An aqueous solution of 15 mol% Gd^{3+} doped $NaYF_4$:Yb/Er (18/2) nanocrystals prepared by the solvothermal treatment for 24 h exhibits the most efficient up-converting luminescence, making them have great superiority for biological applications such as 980-nm laser-driven photovoltaic cells and bio-imaging.

2. Experimental

All of the chemicals used are commercially available and were used as received without further purification. Poly(vinylpyrrolidone) (PVP K30), sodium fluoride, ethylene glycol, and ethanol were purchased from Sinopharm Chemical Reagent Co. (China). Y_2O_3, Yb_2O_3, Er_2O_3 and Gd_2O_3 were obtained from Jinan Henghua Co., China).

$NaYF_4$:Yb/Er nanocrystals with different Gd^{3+} doping concentration were prepared by a solvothermal process with ethylene glycol as the solvent. In a typical synthesis of 15 mol% Gd^{3+} doped $NaYF_4$:Yb/Er, 0.5 mmol (total amounts) of rare earth oxide (0.325 mmol Y_2O_3 + 0.075 mmol Gd_2O_3 + 0.09 mmol Yb_2O_3 + 0.01 mmol Er_2O_3) was dissolved in 10% hydrochloric acid (10 mL), and then the solution was heated to evaporate the water completely. 10 mL ethylene glycol containing 0.5 g PVP was added to dissolve the obtained rare-earth chloride $LnCl_3$ (Ln = Y, Gd, Yb, Er), and the solution was magnetically stirring until a homogeneous solution was formed. Then, 16 mL ethylene glycol colloidal solution containing 7.2 mmol (0.302 g) NaF was injected rapidly into the above solution. The resulting solution was agitated for about 10 min, then transferred to a 30 mL autoclave, sealed, and solvothermally treated at 220 °C for 0–24 h. The system was cooled to room temperature naturally, and white precipitates were collected by centrifugation at 10,000 rpm, and washed with deionized water and ethanol several times to remove impurities. Finally, the precipitates were dried under vacuum at room temperature for 24 h. $NaYF_4$:Yb/Er nanocrystals with different Gd^{3+} doping concentration were synthesized by using the same protocol except that part of Y_2O_3 was replaced by Gd_2O_3.

X-ray diffraction (XRD) measurement was performed on a Bruker D4 X-ray diffractometer using Cu Kα radiation (λ = 0.15418 nm). Sizes and morphologies of samples were determined by using a high-resolution transmission electron microscope (HR-TEM, JEOL JEM-2010F). Fourier transform infrared (FT-IR) spectrum was measured using an IRPRESTIGE-21 spectrometer (Shimadzu) from samples in KBr pellets. Up-converting luminescence spectra were measured by using a JASCO FP-6600 spectrometer, but the excitation source was an external 0–1 W adjustable 980 nm semiconductor laser device with an optic fiber accessory with a diameter of 800 μm (Beijing Hi-Tech Optoelectronic Co., China) instead of the Xenon source in the spectrometer.

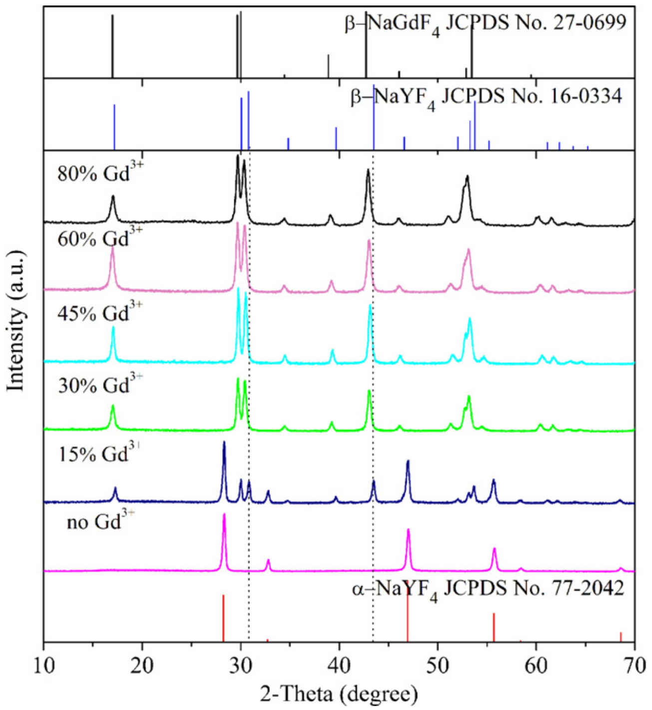

Fig. 1. XRD patterns of $NaYF_4$:Yb/Er samples prepared by the solvothermal treatment at 220 °C for 3 h in the presence of 0, 15, 30, 45, 60 and 80 mol% Gd^{3+} dopant ions, respectively. The standard patterns of cubic phase of $NaYF_4$ and hexagonal phase of $NaYF_4$ and $NaGdF_4$ are also supplied.

3. Results and discussion

3.1. Effects of Gd^{3+} ion concentration

With ethylene glycol as the solvent and PVP as the surfactant, Li and Zhang [27] reported the preparation of $NaYF_4$:Yb/Er nanoparticles by liquid-phase synthesis at 160 °C, but they did not optimize the upconverting luminescence of $NaYF_4$:Yb/Er nanocrystals. In the present work, we investigated the effects of the Gd^{3+} ion doping concentration on the crystal phases, sizes, morphologies and upconverting luminescence of $NaYF_4$:Yb/Er nanocrystals. All these $NaYF_4$:Yb/Er samples in the presence of 0–80 mol% Gd^{3+} dopant ions were prepared by the solvothermal process at 220 °C for 3 h.

Fig. 1 shows X-ray diffraction (XRD) patterns of $NaYF_4$:Yb/Er (18/2 mol%) samples with different Gd^{3+} ion concentration. In the absence of Gd^{3+} ion, XRD pattern of $NaYF_4$:Yb/Er sample can be indexed as the pure cubic (JCPDS file no. 77-2042) phase of $NaYF_4$. Interestingly, the $NaYF_4$:Yb/Er sample in the presence of 15 mol% Gd^{3+} dopant ions is related to a mixture of the cubic and hexagonal phases of $NaYF_4$. The pure hexagonal phase (JCPDS file no. 16-0334) $NaYF_4$ is obtained as Gd^{3+} ion concentration reaches 30 mol%. Thus, the transformation from cubic to hexagonal phase in these $NaYF_4$:Yb/Er samples is evident with the addition of Gd^{3+} ion, which should be attributed to the fact that an increase of Gd^{3+} dopant content in the $NaYF_4$ host favors the formation of hexagonal phase nanocrystals [35]. With further increase of Gd^{3+} ion concentration up to 60 mol%, no extra diffraction peaks are observed, indicating the formation of a homogeneous Y–Gd solid solution [35]. This result should be attributed to the small structural difference between the hexagonal phase $NaYF_4$ (JCPDS no. 16-0334) and $NaGdF_4$ (JCPDS no. 27-0699).

Subsequently, the sizes and morphologies of $NaYF_4$:Yb/Er samples with varying dopant concentration of Gd^{3+} ion were investigated. Fig. 2 shows the typical transmission electron microscope (TEM) images of $NaYF_4$:Yb/Er samples without and with 80 mol%

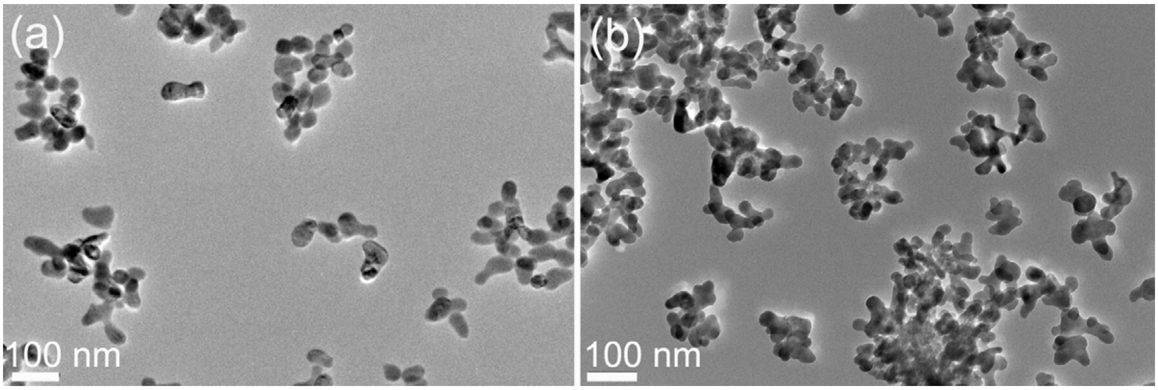

Fig. 2. TEM images of $NaYF_4$:Yb/Er samples (A) without Gd^{3+} dopant ions and (B) with 80 mol% Gd^{3+} dopant ions.

Gd^{3+} dopant ions. All these $NaYF_4$:Yb/Er samples consist of irregular spherical nanoparticles with diameter of 40–100 nm. Thus, no obvious effects of Gd^{3+} ion doping concentration on the sizes and morphologies are observed, which is different from the previous results about the reduction of sizes of $NaYF_4$:Yb/Er nanoparticles arising from Gd^{3+} dopant ions [35], and result from different solvent system. In our case, ethylene glycol as the solvent without addition of water, which is different from oleic acid/ethanol/water solvent system used by Liu et al. [35], may have similar inhibiting effects for the growth of cubic and hexagonal phases of $NaYF_4$, and they also may reduce Gd^{3+} doping-induced size evolution.

Surface functional chemical groups of RUNPs are important for most of their applications [2,3,8]. Herein, the capping ligands on the surface of $NaYF_4$:Yb/Er are identified by FT-IR spectrum (Fig. 3). The as-prepared $NaYF_4$:Yb/Er sample exhibits a broad band at around 3440 cm^{-1}, corresponding to O–H stretching vibration from water molecule. The transmission bands at 2920 and 2851 cm^{-1} are, respectively, assigned to the asymmetric (ν_{as}) and symmetric (ν_s) stretching vibrations of methylene (CH_2) units in PVP and/or ethylene glycol. The bands at 1640 cm^{-1} should be related to a strong C=O adsorption from the lactam group in the side chains of PVP. Based on the above results, it is concluded that there are ethylene glycol and PVP ligands on the surface of $NaYF_4$:Yb/Er samples.

As a result of the presence of ethylene glycol and PVP ligands on their surface, $NaYF_4$:Yb/Er nanoparticles could be readily dispersed in water and in some polar organic solvents such as DMF, or DMSO. Fig. 4A presents the up-converting luminescence spectra of colloidal aqueous solutions containing 1.0 mg/mL $NaYF_4$:Yb/Er nanoparticles with different Gd^{3+} dopant concentration under 980-nm laser excitation. All these spectra are similar to what have been reported previously for these materials [8–21], and they exhibit three distinct Er^{3+} emission bands. The green emissions between 514 and 534 nm and between 534 and 560 nm are attributed to the $^2H_{11/2} \rightarrow {}^4I_{15/2}$ and $^4S_{3/2} \rightarrow {}^4I_{15/2}$ transitions, respectively. A domi-

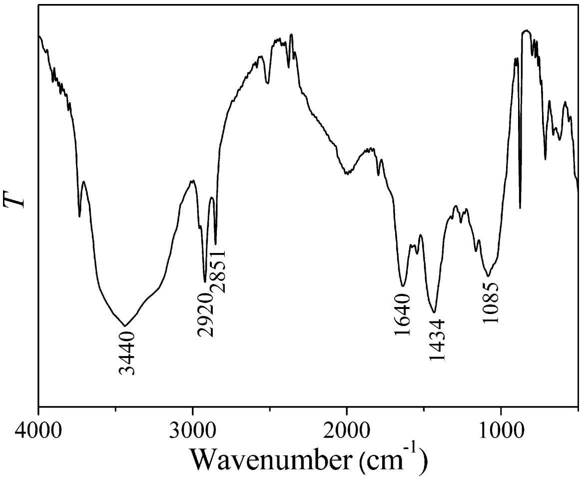

Fig. 3. FTIR spectrum of the $NaYF_4$:Yb/Er nanoparticles.

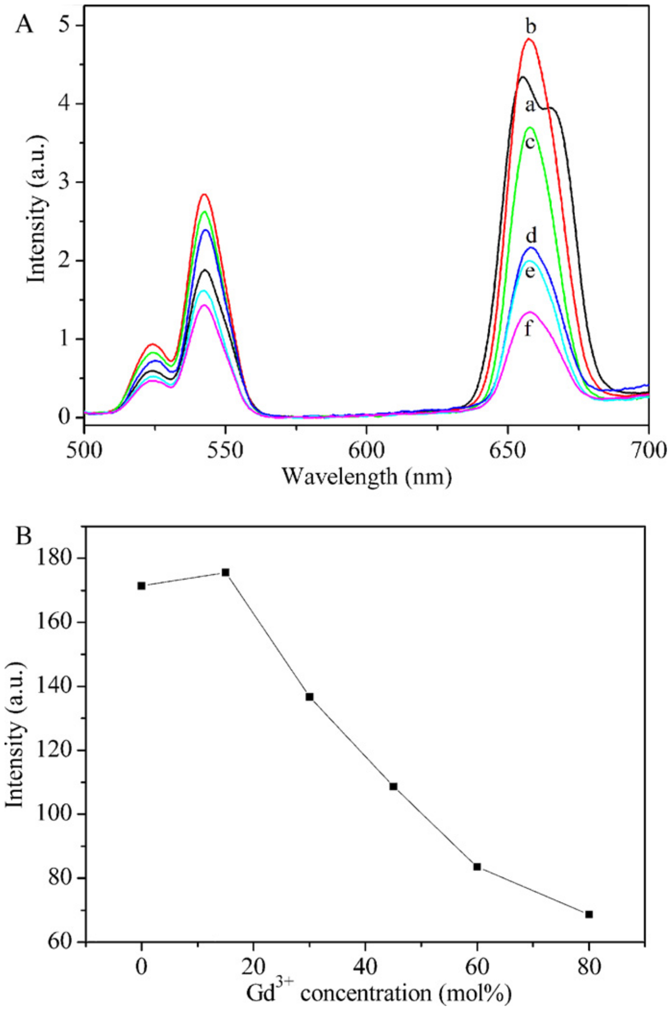

Fig. 4. (A) Luminescence spectra of aqueous solutions of $NaYF_4$:Yb/Er nanoparticles doped with various concentrations of Gd^{3+} ions under continuous-wave excitation of 980 nm laser: (a) no Gd^{3+}, (b) 15 mol% Gd^{3+}, (c) 30 mol% Gd^{3+}, (d) 45 mol% Gd^{3+}, (e) 60 mol% Gd^{3+} and (f) 80 mol% Gd^{3+}. (B) Upconversion emission intensity calculated from the area of emission peaks versus dopant concentration of Gd^{3+} (0–80 mol%).

nant red emission is observed between 635 and 680 nm due to the transition from $^4F_{9/2}$ to $^4I_{15/2}$ (For interpretation of the references to color in this figure, the reader is referred to the web version of the article.).

It is clear that Gd^{3+} dopant concentration has a strong effect on the luminescent intensity of $NaYF_4$:Yb/Er samples. As shown in Fig. 4B, the luminescent intensity, which is calculated from the area of emission peaks, goes up with the increase of Gd^{3+} dopant concentration to 15 mol%, and then exhibits a gradual decrease upon further increase of Gd^{3+} dopant concentration to 80 mol%. This phenomenon is consistent with the previous results, and the initial increase of luminescent efficiency should be attributed to the enhancement of relative amount of hexagonal phase $NaYF_4$ [35]. However, in our case, all these $NaYF_4$:Yb/Er samples have similar shapes and sizes, thus the subsequent decrease of luminescent efficiency cannot be associated with the change of sizes of $NaYF_4$:Yb/Er samples, which is different from the previous results [35]. This decrease should be attributed to the use of $NaGdF_4$ as the host material which is inefficient compared with even cubic phase $NaYF_4$. For example, luminescent intensity of cubic phase $NaYF_4$:Yb/Er without Gd^{3+} doping is almost 2.5 times as strong as that of hexagonal phase $NaGdF_4$:Yb/Er (namely $NaYF_4$:Yb/Er sample with 80 mol% Gd^{3+}).

3.2. Effect of solvothermal time

Obviously, $NaYF_4$:Yb/Er nanoparticles with 15 mol% Gd^{3+} dopant concentration exhibit the highest up-converting luminescent intensity among these samples prepared by the solvothermal process at 220 °C for 3 h. In order to further improve the luminescent efficiency, we investigated the effects of solvothermal time on the crystal phases, sizes, morphologies and upconverting luminescence of $NaYF_4$:Yb/Er nanocrystals. These $NaYF_4$:Yb/Er samples in the presence of 15 mol% Gd^{3+} dopant ions were fabricated by the solvothermal process at 220 °C for 3–24 h.

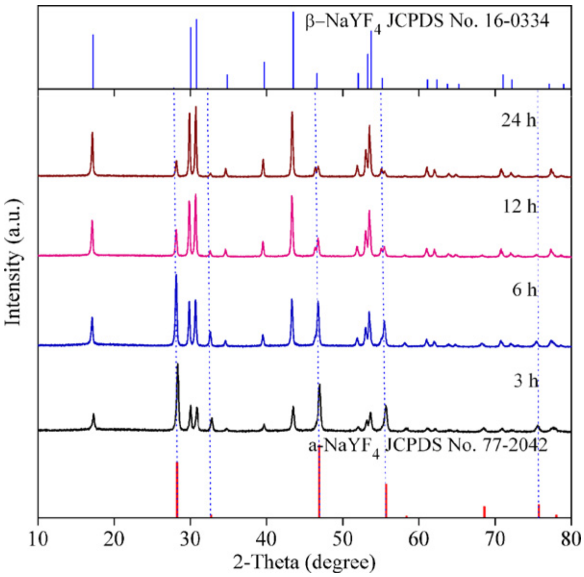

Fig. 5. XRD patterns of 15 mol% Gd^{3+} doped $NaYF_4$:Yb/Er samples fabricated by the solvothermal process at 220 °C for 3–24 h.

Fig. 5 shows XRD patterns of $NaYF_4$:Yb/Er samples prepared by the solvothermal process for different time. The diffraction peak positions and intensities confirm the existence of both cubic (JCPDs card 77-2042) and hexagonal (JCPDs card 16-0334) phase $NaYF_4$. When solvothermal time is 3 h, 15 mol% Gd^{3+} doped $NaYF_4$:Yb/Er sample exhibits dominant cubic phase accompanied by small amounts of hexagonal phase. With the increase of solvothermal time, the relative intensity of cubic phase $NaYF_4$ goes down while that of hexagonal phase $NaYF_4$ goes up, indicating the enhancement of relative amount of hexagonal phase. At last, the sample prepared for 24 h exhibits dominant hexagonal phase accompanied by small amounts of cubic phase. Therefore, it can be concluded that the

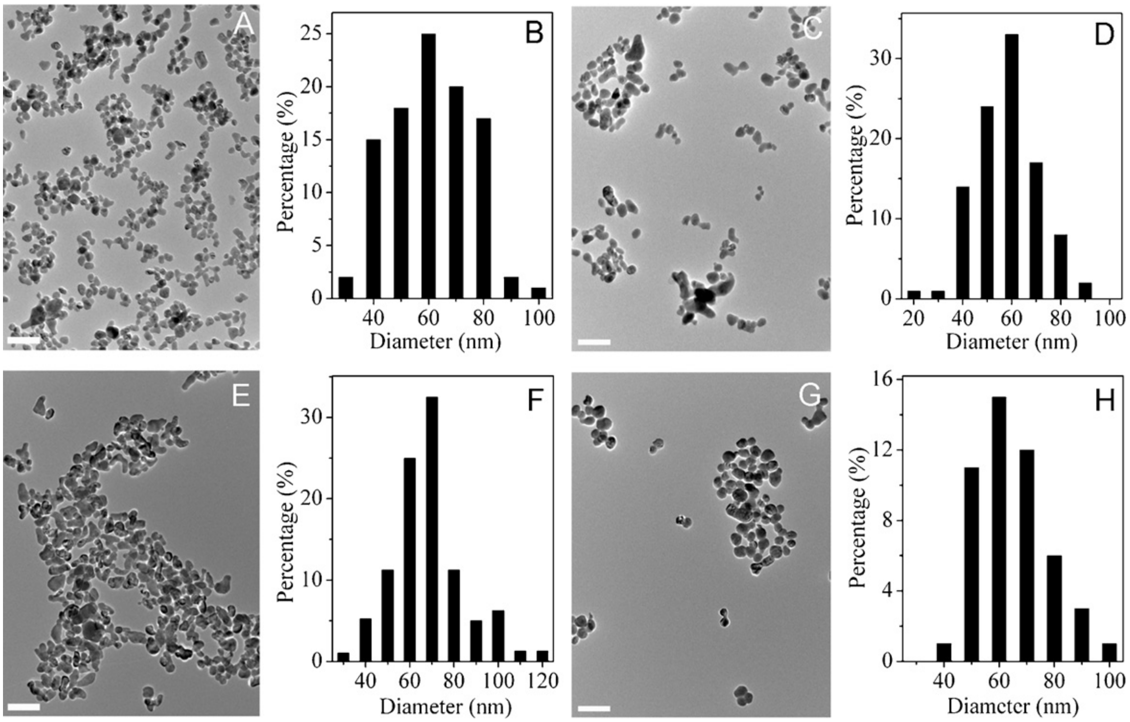

Fig. 6. TEM images and particle size distribution plots of 15 mol% Gd^{3+} doped $NaYF_4$:Yb/Er samples fabricated by the solvothermal process for different solvothermal time: (A, B) 3 h, (C, D) 6 h, (E, F) 12 h, and (G, H) 24 h. Scale bar = 200 nm.

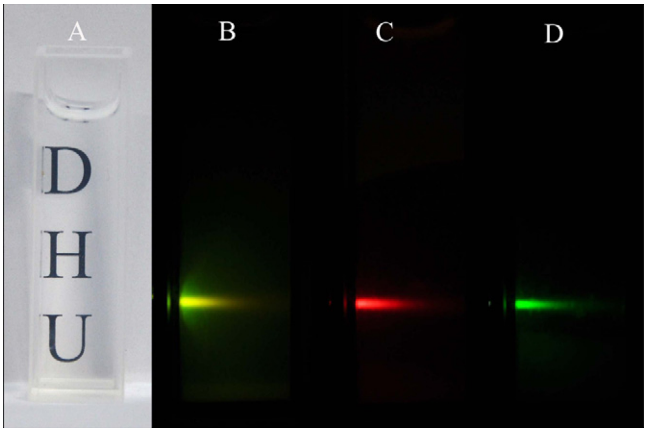

Fig. 7. Colloidal aqueous solutions of 15 mol% Gd^{3+} doped $NaYF_4$:Yb/Er nanocrystals prepared for 24 h: (A) the solution showing its transparency; (B) total upconversion under continuous-wave excitation at 980 nm; (C and D) upconversion viewed through red and green filters, respectively. (For interpretation of the references to color in this figure legend, the reader is referred to the web version of the article.)

increase of solvothermal time favors the formation of hexagonal phase $NaYF_4$:Yb/Er samples.

The effects of the solvothermal time on the sizes and shapes of the as-prepared 15 mol% Gd^{3+} doped $NaYF_4$:Yb/Er samples have been studied by TEM images (Fig. 6). All these samples prepared by the solvothermal treatment for 3–24 h are composed of irregular nanoparticles with diameters of 40–100 nm, and the median diameter is about 60 nm, which shows a relatively broad size distribution. Solvothermal time has no obvious effects on the size and shape of the samples, although it can affect their crystal phase. This may result from that ethylene glycol as the solvent inhibits the further growth of the nanoparticles.

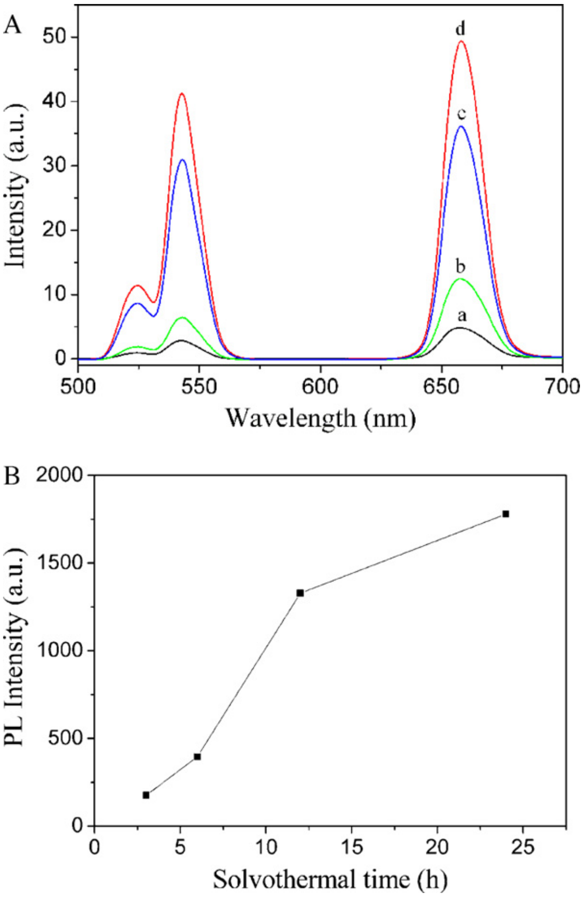

Fig. 8. (A) Luminescent spectra of aqueous solutions of 15 mol% Gd^{3+} doped $NaYF_4$:Yb/Er samples prepared for different reaction time: (a) 3 h, (b) 6 h, (c) 12 h and (d) 24 h. (B) Upconversion emission intensity calculated from the area of emission peaks versus solvothermal time (3–24 h).

Similarly, all these 15 mol% Gd^{3+} doped $NaYF_4$:Yb/Er samples prepared for different solvothermal time could be readily dispersed in water due to the presence of ethylene glycol and PVP ligands on their surface, as shown in Fig. 7A. Fig. 8A shows the up-converting luminescence spectra of colloidal aqueous solutions containing 1.0 mg/mL 15 mol% Gd^{3+} doped $NaYF_4$:Yb/Er samples under 980-nm laser excitation. All these spectra exhibit three distinct Er^{3+} emission bands, which are similar to the previous reports. Interestingly, both the green and red emission intensities go up rapidly with the increase of solvothermal time from 3 to 24 h, which should be attributed to the enhancement of relative amount of hexagonal phase $NaYF_4$ as revealed in Fig. 5 (For interpretation of the references to color in this figure, the reader is referred to the web version of the article.). It is clear that the nanoparticles prepared for 24 h exhibit the highest upconverting luminescence intensity (Fig. 8B), which is almost 11 times as strong as that of ones prepared for 3 h and almost 28 times as strong as that of hexagonal phase $NaGdF_4$:Yb/Er (namely $NaYF_4$:Yb/Er sample with 80 mol% Gd^{3+} prepared for 3 h). The total luminescence (Fig. 7B) of 15 mol% Gd^{3+} doped $NaYF_4$:Yb/Er nanoparticles prepared for 24 h appears bright yellow-green in color due to a combination of red and green emissions from the Er^{3+} ion. This is confirmed by Fig. 7C and D, where the solution under the same excitation conditions is viewed through red and green filters, respectively. Since all these samples have similar sizes and shapes, 15 mol% Gd^{3+} doped $NaYF_4$:Yb/Er sample prepared for 24 h has great superiority as luminescent materials due to its highest luminescence efficiency.

4. Conclusions

Hydrophilic Gd^{3+} doped $NaYF_4$:Yb/Er nanoparticles with diameters of 40–100 nm have been prepared by a one-pot solvothermal synthesis with ethylene glycol as the solvent and PVP as the ligands at 220 °C for different time. Gd^{3+} doping concentration and reaction time has no obvious effects on their sizes but have strong effects on their phase and luminescent intensity. The increase of Gd^{3+} doping content favors the transformation from cubic to hexagonal phase, and Gd^{3+} doping content at 15 mol% results in high up-converting luminescence efficiency. Longer reaction time leads to higher luminescence efficiency, and an aqueous solution of 15 mol% Gd^{3+} doped $NaYF_4$:Yb/Er (18/2) nanocrystals prepared for 24 h exhibits the most efficient up-converting luminescence. This 15 mol% doped $NaYF_4$:Yb/Er sample has great superiority for biological applications due to its small size (40–100 nm), high hydrophilicity and excellent up-converting luminescence.

Acknowledgements

The authors thank Prof. Xiaogang Liu (*Department of Chemistry, National University of Singapore*) for helpful comments and suggestion. This work was financially supported by the Program for New Century Excellent Talents of the University in China, the National Natural Science Foundation of China (Grant Nos. 50872020 and 50902021), the “Pujiang” Program of Shanghai Education Commission in China (Grant No. 09PJ1400500), the “Dawn” Program of Shanghai Education Commission in China (Grant No. 08SG32), Specialized Research Fund for the Doctoral Program of Higher Education (Grant No. 20090075120014), “Chen Guang” project (Grant No. 09CG27) supported by Shanghai Municipal Education Commission and Shanghai Education Development Foundation, Shanghai

Leading Academic Discipline Project (Grant No. B603), the Fundamental Research Funds for the Central Universities, and the Program of Introducing Talents of Discipline to Universities (Grant No. 111-2-04).

References

[1] F. Auzel, Chem. Rev. 104 (2004) 139.
[2] F. Wang, X.G. Liu, Chem. Soc. Rev. 38 (2009) 976.
[3] F. Wang, D. Banerjee, Y.S. Liu, X.Y. Chen, X.G. Liu, Analyst 135 (2010) 1839.
[4] T. Liu, Z.M. Yang, S.H. Xu, Opt. Exp. 17 (2009) 235.
[5] E. Downing, L. Hesselink, J. Ralston, R. Macfarlane, Science 273 (1996) 1185.
[6] V. Badescu, J. Appl. Phys. 104 (2008) 113120.
[7] F. Kaczmarek, Z. Stryla, A. Jendrzejczak, Appl. Phys. B: Laser Opt. 73 (2001) 125.
[8] Z.G. Chen, H.L. Chen, H. Hu, M.X. Yu, F.Y. Li, Q. Zhang, Z.G. Zhou, T. Yi, C.H. Huang, J. Am. Chem. Soc. 130 (2008) 3023.
[9] Z.G. Chen, L.S. Zhang, Y.G. Sun, J.Q. Hu, D.Y. Wang, Adv. Funct. Mater. 19 (2009) 3815.
[10] L.Y. Wang, Y.D. Li, Chem. Mater. 19 (2007) 727.
[11] X. Wang, J. Zhuang, Q. Peng, Y.D. Li, Inorg. Chem. 45 (2006) 6661.
[12] X. Wang, J. Zhuang, Q. Peng, Y.D. Li, Nature 437 (2005) 121.
[13] F. Zhang, Y. Wan, T. Yu, F.Q. Zhang, Y.F. Shi, S.H. Xie, Y.G. Li, L. Xu, B. Tu, D.Y. Zhao, Angew. Chem. Int. Ed. 46 (2007) 7976.
[14] H.X. Mai, Y.W. Zhang, R. Si, Z.G. Yan, L.D. Sun, L.P. You, C.H. Yan, J. Am. Chem. Soc. 128 (2006) 6426.
[15] G.S. Yi, G.M. Chow, Adv. Funct. Mater. 16 (2006) 2324.
[16] J.C. Boyer, F. Vetrone, L.A. Cuccia, J.A. Capobianco, J. Am. Chem. Soc. 128 (2006) 7444.
[17] S. Heer, K. Kömpe, H.U. Güdel, M. Haase, Adv. Mater. 16 (2004) 2102.
[18] O. Lehmann, H. Meyssamy, K. Kömpe, H. Schnablegger, M. Haase, J. Phys. Chem. B 107 (2003) 7449.
[19] S. Heer, O. Lehmann, M. Haase, H.U. Güdel, Angew. Chem. Int. Ed. 42 (2003) 3179.
[20] C.H. Liu, H. Wang, X.R. Zhang, D.P. Chen, J. Mater. Chem. 19 (2009) 489.
[21] Z.Q. Li, Y. Zhang, S. Jiang, Adv. Mater. 20 (2008) 4765.
[22] G.S. Yi, G.M. Chow, Chem. Mater. 19 (2007) 341.
[23] L.Y. Wang, R.X. Yan, Z.Y. Hao, L. Wang, J.H. Zeng, H. Bao, X. Wang, Q. Peng, Y.D. Li, Angew. Chem. Int. Ed. 44 (2005) 6054.
[24] F. Wang, D.K. Chatterjee, Z. Li, Y. Zhang, X.P. Fan, M.Q. Wang, Nanotechnology 17 (2006) 5786.
[25] M. Wang, C.C. Mi, J.L. Liu, X.L. Wu, Y.X. Zhang, W. Hou, F. Li, S.K. Xu, J. Alloys Compd. 485 (2009) L24.
[26] L.Q. Xiong, Z.G. Chen, M.X. Yu, F.Y. Li, C. Liu, C.H. Huang, Biomaterials 30 (2009) 5592.
[27] Z.Q. Li, Y. Zhang, Angew. Chem. Int. Ed. 45 (2006) 7732.
[28] Z.G. Chen, Q.W. Tian, Y.L. Song, J.M. Yang, J.Q. Hu, J. Alloys Compd. 506 (2010) L17.
[29] F. Zhang, Y. Deng, Y.F. Shi, R.Y. Zhang, D.Y. Zhao, J. Mater. Chem. 20 (2010) 3895.
[30] Z.L. Wang, J.H. Hao, H.L.W. Chan, J. Mater. Chem. 20 (2010) 3178.
[31] F. Vetrone, R. Naccache, V. Mahalingam, C.G. Morgan, J.A. Capobianco, Adv. Funct. Mater. 19 (2009) 2924.
[32] F. Wang, J. Wang, X.G. Liu, Angew. Chem. Int. Ed. 49 (2010) 7456.
[33] K.W. Krämer, D. Biner, G. Frei, H.U. Güdel, M.P. Hehlen, S.R. Lüthi, Chem. Mater. 16 (2004) 1244.
[34] C.X. Li, J. Yang, Z.W. Quan, P.P. Yang, D.Y. Kong, J. Lin, Chem. Mater. 19 (2007) 4933.
[35] F. Wang, Y. Han, C.S. Lim, Y.H. Lu, J. Wang, J. Xu, H.Y. Chen, C. Zhang, M.H. Hong, X.G. Liu, Nature 463 (2010) 1061.
[36] R.A. Jalil, Y. Zhang, Biomaterials 29 (2008) 4122.